Crystal structures of cobalamin-independent methionine synthase complexed with zinc, homocysteine, and methyltetrahydrofolate

Jean-Luc Ferrer, Stephane Ravanel, Mylène Robert, Renaud Dumas

▶ To cite this version:

HAL Id: hal-02678195
https://hal.inrae.fr/hal-02678195

Submitted on 31 May 2020

Accelerated Publication

Crystal Structures of Cobalamin-independent Methionine Synthase Complexed with Zinc, Homocysteine, and Methyltetrahydrofolate*S◆

**Jean-Luc Ferrer‡§, Stéphane Ravanel¶,
Mylène Robert¶, and Renaud Dumas¶‖**

*From the ‡Laboratoire de Cristallogenèse et
Cristallographie des Protéines, Institut de Biologie
Structurale J.-P. Ebel, 41 rue Jules Horowitz, 38027
Grenoble cedex 1, France and the ¶Laboratoire de
Physiologie Cellulaire Végétale, CEA-Grenoble, 17 rue
des Martyrs, 38054, Grenoble cedex 9, France*

Cobalamin-independent methionine synthase (MetE)
catalyzes the synthesis of methionine by a direct trans-
fer of the methyl group of N^5-methyltetrahydrofolate
(CH_3-H_4PteGlu$_n$) to the sulfur atom of homocysteine
(Hcy). We report here the first crystal structure of this
metalloenzyme under different forms, free or complexed
with the Hcy and folate substrates. The *Arabidopsis
thaliana* MetE (AtMetE) crystals reveal a monomeric
structure built by two $(\beta\alpha)_8$ barrels making a deep
groove at their interface. The active site is located at the
surface of the C-terminal domain, facing the large inter-
domain cleft. Inside the active site, His^{647}, Cys^{649}, and
Cys^{733} are involved in zinc coordination, whereas
Asp^{605}, Ile^{437}, and Ser^{439} interact with Hcy. Opposite the
zinc/Hcy binding site, a cationic loop (residues 507–529)
belonging to the C-terminal domain anchors the first
glutamyl residue of CH_3-H_4PteGlu$_5$. The pterin moiety of
CH_3-H_4PteGlu$_5$ is stacked with Trp^{567}, enabling the N^5-
methyl group to protrude in the direction of the zinc
atom. These data suggest a structural role of the N-
terminal domain of AtMetE in the stabilization of loop
507–529 and in the interaction with the poly-glutamate
chain of CH_3-H_4PteGlu$_n$. Comparison of AtMetE struc-
tures reveals that the addition of Hcy does not lead to a
direct coordination of the sulfur atom with zinc but to a
reorganization of the zinc binding site with a stronger
coordination to Cys^{649}, Cys^{733}, and a water molecule.

In all organisms, the sulfur-containing amino acids homocys-
teine (Hcy)[1] and methionine (Met) are situated at a point of
convergence of two major metabolic networks, *i.e.* sulfur and
one-carbon metabolisms. Four enzymes are capable of synthe-
sizing Met by methylation of the thiol group of Hcy using
different methyl group donors. First, two types of the enzyme
Met synthase catalyze the same overall reaction, the transfer of
the methyl group of N^5-methyltetrahydropteroylglutamate
(CH_3-H_4PteGlu) to Hcy (1). The cobalamin-dependent Met syn-
thase (EC 2.1.1.13, MetH) is found in organisms that synthe-
size or obtain vitamin B_{12} from outside sources (*e.g.* bacteria
and animals). MetH is a large modular protein in which the
methyl group of CH_3-H_4PteGlu is first transferred to an en-
zyme-bound cobalamin co-factor and then captured by Hcy (for
a review, see Ref. 2). MetH is a monomeric protein composed of
four regions with the N-terminal part comprising modules for
binding and activation of Hcy and CH_3-H_4PteGlu and the C-
terminal half containing the cobalamin and *S*-adenosylmethi-
onine binding domains (2). The cobalamin-independent Met
synthase (EC 2.1.1.14, MetE) shares no sequence similarity
with MetH (1) and catalyzes methyl transfer to Hcy directly
from CH_3-H_4PteGlu$_n$ (with $n > 3$). Both MetE and MetH are
found in bacteria, whereas fungi and plants possess only the
cobalamin-independent Met synthase (3, 4). Second, the en-
zymes betaine Hcy *S*-methyltransferase (EC 2.1.1.5; BHMT)
and *S*-methylmethionine Hcy *S*-methyltransferase (EC
2.1.1.12; HMT) use the methyl groups of betaine and *S*-meth-
ylmethionine, respectively, to methylate Hcy. BHMT occurs in
mammals (5) and in halophylic bacteria (6). HMT is found in
plants, bacteria, fungi, and mammals, enabling these organ-
isms to utilize *S*-methylmethionine of plant origin (7, 8).

All the above mentioned enzymes catalyzing methyl trans-
fers to thiols contain a zinc atom that is essential for binding of
Hcy and for catalysis of methyl transfer to the Hcy thiolate (9).
Recent crystal structure determinations (10–12) established
that MetH, BHMT, and HMT share a homologous N-terminal
Hcy binding domain (Hcy *S*-methyltransferase family pfam
PF02574) in which a zinc atom is linked to three cysteine
residues (in bold) included in two conserved motifs, G(I/L/V)N**C**
and (I/V)GG**CC**(G/R), and to a fourth oxygen or nitrogen ligand
(tyrosine or threonine residues in BHMT and MetH, respec-
tively). MetE belongs to a distinct family of zinc metalloenzymes
(9). Indeed, although the structure of MetE was still unknown,
site-directed mutagenesis and analyses of the zinc environment
by extended x-ray absorption fine structure (EXAFS) led to the
identification of the zinc and Hcy binding domain in the C-
terminal of the *Escherichia coli* enzyme (13, 14).

Although the zinc ligand set of the *E. coli* enzyme has been
characterized, further investigations are needed to get a better
understanding of the role of zinc in direct methyl transfer from
CH_3-H_4PteGlu$_n$ to Hcy. In the present paper, we report the
first three-dimensional structure of a cobalamin-independent
Met synthase from the higher plant *Arabidopsis thaliana* (At-

---

MetE). Cocrystallization of the enzyme in the presence of zinc and, with or without, Hcy or Met permitted determination of the zinc binding site and its interactions with the substrate and product, respectively. Furthermore, crystal soaking with CH_3-$H_4PteGlu_n$ led to the identification of the binding site of the methyl donor.

EXPERIMENTAL PROCEDURES

Protein Expression and Purification—Protein expression was carried out with plasmid pET-MS1 encoding the full-length AtMS1 cytosolic enzyme (4). *E. coli* BL21-codonPlus (DE3)-RIL-X cells carrying the pET-MS1 plasmid were grown at 28 °C in 1 liter of LB medium containing 0.5 mM $ZnSO_4$ until A_{600} reached 0.6. Isopropyl β-D-thiogalactoside was added to a final concentration of 0.4 mM, and the cells were further grown for 15 h at 28 °C. Cells were harvested by centrifugation, and the pellet was resuspended in 50 ml of buffer A (10 mM KH_2-K_2HPO_4, pH 7.2, 1 mM DTT) and sonicated. The soluble AtMetE protein was purified by ion-exchange chromatography on a Fractogel® EMD DEAE column using a KH_2-K_2HPO_4 linear gradient (10–100 mM). Pure enzyme was concentrated to 20 mg of protein/ml in 20 mM KH_2-K_2HPO_4, pH 7.2, 1 mM DTT, and stored at -80 °C until used. The seleno-Met enzyme (Se-AtMetE) was expressed and purified similarly except that the growth was conducted in 1 liter of a minimal medium containing 40 mg of seleno-Met. The native molecular mass of AtMetE was determined on a Superdex 200 16/60 equilibrated in 50 mM Tris-HCl, pH 8.0, and 150 mM KCl. AtMetE was eluted as a monomer of 84 kDa, as expected from its theoretical molecular mass.

Crystallization of AtMetE—Crystals (space group $P6_5$) were grown at 20 °C in 12-μl sitting drops containing 6 μl of protein mix (30 μg of AtMetE or Se-AtMetE, 1 mM DTT, 1 mM $ZnCl_2$, 10 mM L-Met or L-Hcy) and 6 μl of reservoir solution. For crystals obtained in the presence of Met or Hcy, 3% (w/v) saccharose or 3% (w/v) glycerol were added to the protein mix, respectively. For these crystals, the reservoir solution consisted of 30% (w/v) polyethylene glycol (PEG) 8000, 0.2 M ammonium sulfate, 1 mM DTT, and 0.1 M sodium cacodylate, pH 6.5. For crystals grown without Met or Hcy, 0.1 M ammonium sulfate was added to the protein mix, and the reservoir solution consisted of 0.1 M Tris-HCl, pH 8.5, 32% (w/v) PEG 4000, 0.2 M lithium sulfate. Soaking experiments were performed by adding 10 mM of pteroylpenta-γ-L-glutamate (PteGlu$_5$, Schircks Laboratories) or CH_3-$H_4PteGlu_5$ (synthesized from PteGlu$_5$ as described by Ravanel *et al.* (4)) in the crystallization drop. Cryo-conditions consisted of 5% (w/v) glycerol, 1 mM $ZnCl_2$, 1 mM DTT, 10 mM Met/Hcy/PteGlu$_5$/CH_3-$H_4PteGlu_5$ added to the reservoir solution.

Structure Determination—The structure of Met-complexed Se-AtMetE was determined by single wavelength anomalous diffraction. Data (data set Se-Met, see Supplemental Table I) were collected at the selenium K edge (wavelength: 0.9792 Å) at 100 K on FIP-BM30A (15) beamline at the European Synchrotron Radiation Facility and reduced with XDS (16). Data were input to SOLVE (17), which found 17 sites (mean figure of merit: 0.26) out of the 19 anticipated selenium sites. Density modification was performed in RESOLVE (mean figure of merit: 0.66; Ref. 18), and 121 residues out of 765 were build automatically. The model was extended to a total of 746 residues (residues 1 and 418–460 were not observed in the electronic density) by manual building using the O molecular modeling package (19). This model was refined in CNS (20) using torsional simulated annealing, followed by refinement of atomic B factors and least squares minimization. Water molecules were gradually added to the model at positions where density difference was higher than 2.5 σ, provided they make acceptable interactions with protein atoms or other water molecules. This final model was also refined against the data set (supplemental Table I) collected on crystals obtained, either by co-crystallization or by soaking, in the presence of different substrates or products: Met, Hcy, PteGlu$_5$, and CH_3-$H_4PteGlu_5$ (data sets: Met, Hcy, Se-Hcy, Se-Met-PteGlu$_5$, Se-Hcy-PteGlu$_5$, Se-Met-CH_3-$H_4PteGlu_5$). One data set was also collected on a seleno-Met derivative crystal obtained without Met or Hcy added during crystallization (data set Se-Free). This last crystal was obtained in a rather different crystallization condition with respect to the other ones but happened to grow in the same space group, with similar cell parameters. Some of these crystals presented a hemihedral twining, ranging from 3.5 to 18%, and refinement steps were performed accordingly (21).

RESULTS AND DISCUSSION

Overall Structure—AtMetE crystals revealed a monomeric structure in agreement with gel filtration chromatography (see "Experimental Procedures"). The monomer is built by two do-
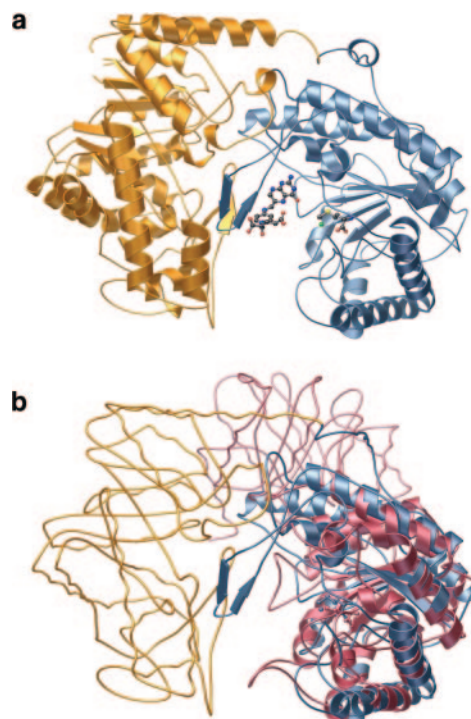

FIG. 1. **Structure of the *Arabidopsis* MetE.** *a*, ribbon diagram of AtMetE in complex with Met and PteGlu$_5$. The Met and PteGlu$_5$ molecules are depicted as *sticks* and *balls*. The N-terminal domain is *gold*, the C-terminal domain is *blue*, and the zinc atom is *green*. *b*, structural alignment with the Hcy domain of MetH (in *pink*, code 1Q8A in the Protein Data Bank) performed with DALI. Secondary structures are shown only for residues 416–792 for AtMetE. Diagrams were produced with MOLSCRIPT (22) and rendered with POV-RAY (www.povray.org).

mains making a deep groove at their interface (Fig. 1*a*). The N-terminal domain extends from residues 2 to 391 and the C-terminal domain from residues 392 to 765. Both are structurally similar to the classical $(\beta\alpha)_8$ barrel as represented by uroporphyrinogen decarboxylase (code 1URO in the Protein Data Bank). Structural alignment performed with DALI (www.ebi.ac.uk/dali/fssp/) gives a root mean square distance (r.m.s.d.) to 1URO of 3.1 and 3.3 Å, for the N- and C-terminal domains, respectively. Both domains are also structurally similar to the Hcy binding domain of MetH (code 1Q8A in the Protein Data Bank), with a r.m.s.d. of 3.3 and 3.5 Å, respectively (Fig. 1*b*). The linker between the two domains consists of a loop (residues 390–395). A large loop of the C-terminal domain including β strands $\beta12$, $\beta13$, $\beta14$, and $\beta15$ (residues 507–529) crosses over the groove and closely interacts with the N-terminal domain. Inside the groove, the C-terminal domain seems to be involved in the interaction with zinc, Hcy/Met, and CH_3-$H_4PteGlu_5$ (Fig. 1). This result contrasts markedly with the MetH enzyme in which Hcy, CH_3-$H_4PteGlu$, and cobalamin binding sites belong to three different domains (12).

Zinc Binding Site—Two zinc atoms were observed in the electronic density of all the collected data set. One is located at the interface between two AtMetE molecules, making bonds with His[658] and Asp[662] from one molecule and His[135] and Asp[194] from the other molecule. This metal atom does not appear to have any catalytic role. The other zinc atom is located in the active site, at the surface of the C-terminal domain, in the groove that separates the two domains (Fig. 1*a*). The nature of these ions is assumed based on the absence of any other heavy atom, except selenium and arsenic, as detected by fluorescence spectrum measurements performed on the crystals with a multi-channel detector (see supplementary Fig. 1*a*). This point was also established undoubtedly by collecting a
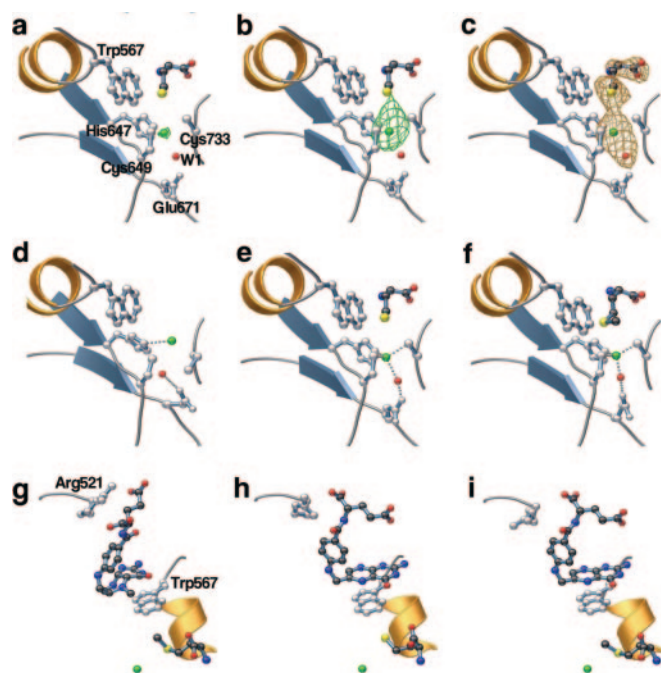
FIG. 2. **Close-up view of the AtMetE active site.** An anomalous difference Fourier density map of AtMetE complexed with Hcy, below (*a*) and above (*b*) the zinc K absorbtion edge, contoured at 6 σ is shown. In comparison with the Fourier difference map (*c*) calculated with phases from the AtMetE model and contoured at 4 σ, only one part of the elongated density at the ion position appears to be zinc, suggesting the presence of a water molecule, W1. *d–f*, zinc coordinating residues of free AtMetE (*d*), complexed with Hcy (*e*), and complexed with Met (*f*). *g–i*, methyl donor binding site of AtMetE complexed with Met and CH_3-H_4PteGlu$_5$ (*g*), Hcy and PteGlu$_5$ (*h*), and Met and PteGlu$_5$ (*i*). Zinc is shown in *green* and W1 in *red*. Diagrams were produced with MOLSCRIPT/BOBSCRIPT (22) and rendered with POV-RAY (www.povray.org).

FIG. 3. **Charge colored surface of the methyl donor binding site.** This figure, showing AtMetE complexed with CH_3-H_4PteGlu$_5$ and Met, was produced with DINO (Visualizing Structural Biology, 2002, www.dino3d.org).

two-wavelength data set (data set Se-Hcy), one above and one below the zinc K absorption edge (see supplementary Fig. 1*b*). The anomalous difference map obtained with phases from the refined model shows a strong peak above the edge at the assumed ion location (28 σ) that almost disappears below the edge (7 σ, so a ratio of 4:1 close to the variation of the *f'* parameter of zinc between these two wavelengths, see Fig. 2, *a* and *b*). The shape of the anomalous density matches only a part, the half part close to the substrate (see Fig. 2*c*), of the total density observed when calculating a difference density map. It reveals the presence of a water molecule (named W1) in a close position, at about 2–3 Å distance from zinc. W1 makes H-bonds with backbone oxygen of Asp[732], a side chain oxygen of Glu[671], and the sulfur of Cys[733], depending on the presence or not of the ligands (Fig. 2, *d–f*). In addition, the zinc atom binds also to the sulfur atom of Cys[649] and Cys[733] and to the side chain nitrogen of His[647]. This result is in complete agreement with mutagenesis and EXAFS experiments (13, 14) showing that the zinc atom is coordinated in the *E. coli* enzyme to two sulfur ligands (Cys[643] and Cys[726]), to His[641], and to a water molecule. All the residues involved in the binding of the zinc atom and W1 are strictly conserved in the MetE family (see supplemental Fig. 2).

Homocysteine/Methionine Binding Site—Data sets were obtained for the AtMetE protein co-crystallized with either Met or Hcy (supplemental Table I). Met was observed close to the catalytic zinc atom (Fig. 2*f*). The nitrogen atom of Met makes H-bonds with the carboxylate moiety of Asp[605] and the backbone oxygen of Ile[437], whereas oxygen atom makes a H-bond with backbone nitrogen of Ser[439]. Density observed in the active site for crystals grown in the presence of Hcy permitted us
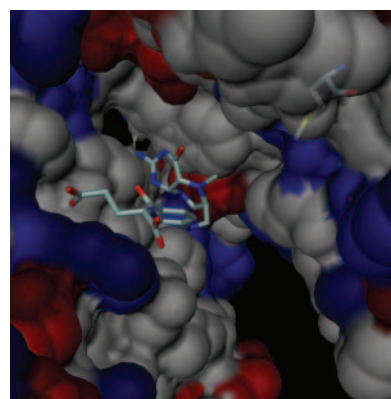
to model the Hcy molecule in a rather similar position than the observed Met (Fig. 2*e*). Refinement revealed a slightly different position of the substrate molecule, with the sulfur of Hcy overlapping carbon C-5 of Met. In both cases, the sulfur atom of Hcy/Met and zinc do not interact strongly (distance S-Zn = 3.6–4.4 Å, see supplemental Table I). The data collected on Se-AtMetE with or without Met added (data sets Se-Met and Se-Free, see supplemental Table I) revealed an electronic density but no anomalous signal at the position of Met (result not shown), suggesting the presence of water molecules in the case of data set Se-Free (Fig. 2*d*). It proves that no seleno-Met was kept from the cells where AtMetE was produced. Except for Ile[437] (replaced by Val in the sequence of *Methanobacterium thermoautotrophicum*), all the residues involved in the binding of Met/Hcy are rigorously conserved in the MetE family (see supplemental Fig. 2).

Folate Binding Site—When crystals of AtMetE complexed with Met or Hcy were soaked with PteGlu$_5$ or CH_3-H_4PteGlu$_5$, a new density was observed on the opposite side of the groove with respect to the zinc catalytic atom. Only the pterin ring and the first glutamyl residue of PteGlu$_5$ and CH_3-H_4PteGlu$_5$ were successfully modeled in the corresponding density. A weaker density was also observed for the *p*-aminobenzoate moiety, suggesting the possibility of a free rotation of the ring. In both cases, the glutamyl residue is bound in a positively charged binding pocket (loop 507–529) (Fig. 3), with ionic and H-bond interactions with the side chain of Arg[521] and the backbone oxygen of Cys[522], respectively. The pterin ring of PteGlu$_5$/CH_3-H_4PteGlu$_5$ protrudes in the direction of the zinc atom, making only a stacking interaction with Trp[567] (Fig. 2, *g–i*). These interactions are similar for PteGlu$_5$ and CH_3-H_4PteGlu$_5$, but due to the nonaromatic nature of the pterin ring of CH_3-H_4PteGlu$_5$, its general shape (Fig. 2*g*) differs substantially from PteGlu$_5$, making atom N^5 of the pterin ring come closer to the zinc atom with respect to PteGlu$_5$ (Fig. 2, *h* and *i*). At this position, the distance between the methyl to be transferred from CH_3-H_4PteGlu$_5$ to the sulfur of Hcy is about 7 Å. As observed for AtMetE, most of the crystal structures of folate-requiring enzymes have been determined without the polyglutamate chain or having only a single glutamyl residue (23). This deficiency is not due to a hydrolysis of folate but could be inherent of the nature of the anionic polyglutamate chain. Indeed, the enzymes are often crystallized in high salt concentrations, and the anions of these salts compete for binding with the anionic polyglutamate chain (23). In addition, it is also possible that the polyglutamate chain of folate has several conformations preventing its determination from an electron density map (23).

Although only one glutamyl residue is observed in the structure, the length of the polyglutamate chain is of critical importance for enzyme activity, CH_3-H_4PteGlu$_1$ being a poor substrate of the plant and bacterial MetE enzymes (4, 24, 25). Also, binding studies with the *E. coli* MetE enzyme demonstrated that the length of the polyglutamate chain markedly increases the binding of the folate substrate (26). In agreement with these data, soaking of the AtMetE crystals with CH_3-H_4PteGlu$_1$ did not permit us to identify a density at the position determined for CH_3-H_4PteGlu$_5$ (results not shown). As suggested by cationic surface charge distribution (Lys[14], Arg[15], Asn[339]) (Fig. 3), the function of the N-terminal domain would be to interact with the negatively charged polyglutamate chain of CH_3-H_4PteGlu$_5$. In addition, considering the close interactions of loop 507–529 with the N-terminal domain and the lack of interaction with the C-terminal domain, we can assume also that the role of the N-terminal domain is to stabilize the loop 507–529.

It is worth noting that the MetE protein from the methane-forming archaeon *M. thermoautotrophicum* shares a high sequence similarity with MetE from *E. coli* and higher plants, including loop 507–529 and residues involved in the zinc and Hcy binding sites, but does not contain the N-terminal domain (see supplemental Fig. 2). Surprisingly, neither CH_3-H_4PteGlu nor its analog N^5-methyltetrahydromethanopterin are active methyl donors for Hcy methylation by the archaeal enzyme (27).

Active Site and Reaction Mechanism—Comparisons between the structures of the enzyme with zinc (Se-Free data set) and the complexes with Hcy or Met (Se-Hcy, Hcy, Se-Met, and Met data sets) show that binding of Hcy or Met leads to similar conformational modifications at the zinc binding site (Fig. 2, *d*, *g*, and *h*). Indeed, binding of the Hcy/Met induces (i) a flip of Cys[733] from His[701] to zinc and (ii) a slight displacement (1.2 Å) of zinc leading to a stronger coordination of zinc to Cys[649] (distance Zn-S = 2.4 Å instead of 3.3 Å, see supplemental Table I), Cys[733] (Zn-S = 2.4 Å instead of 3.4 Å), and W1 (Zn-W1 = 2.3 Å instead of 3.5 Å). At the same time, H-bonds between W1 and the sulfur of Cys[733] (Cys[733]-W1 = 3.8 Å instead of 2.7 Å) and the side chain nitrogen of His[647] (His[647]-W1 = 3.7 Å instead of 2.8 Å) disappear in favor of new H-bonds with the backbone oxygen of Asp[732] (Asp[732]-W1 = 2.7 Å instead of 3.5 Å) and with the side chain oxygen of Glu[671] (Glu[671]-W1 = 2.8 Å instead of 3.7 Å). In both cases, the sulfur atom of Hcy/Met replaces a water molecule (W305) at a distance between 3.6 and 4.4 Å from zinc.

Previous experiments carried out with the *E. coli* MetE established already that zinc is coordinated to two cysteines, one histidine, and a water molecule that is exchangeable with the thiol group from Hcy upon substrate binding (14). Thus, it was proposed that (i) direct coordination of zinc to Hcy, two sulfurs (Cys[649], Cys[733]) and one nitrogen (His[647]) atoms, confers a net negative charge to the substrate-zinc complex, (ii) zinc acts as a Lewis acid that activates Hcy in a thiolate that is more reactive than the corresponding thiol, and (iii) the thiolate is a strong nucleophile that further attacks the N^5 of CH_3-H_4PteGlu$_n$ yielding thiol alkylation. Analysis of the zinc binding site of AtMetE complexed with Hcy is not in complete agreement with this hypothesis. Indeed, our results show clearly that the binding of Hcy does not lead to a direct coordination of the sulfur atom to zinc but rather to a reorganization of the zinc binding site, which exhibits stronger interactions with Cys[649], Cys[733], and W1, keeping unmodified the interaction with His[647] (supplemental Table I). Alternatively, another possible mechanism is that coordination of zinc to W1 leads to an hydroxyl, which then activates Hcy in a thiolate.

However, our results are not even in agreement with this mechanism, since the distance between W1 and S(Hcy) is far away (6 Å) to allow thiol activation.

Analyses of the crystal structure of AtMetE soaked with PteGlu$_5$ or CH_3-H_4PteGlu$_5$ indicate that the pterin ring of both pteroyl compounds is stacked against Trp[567]. In the case of CH_3-H_4PteGlu$_5$, the methyl group remains far away from the sulfur atom of Hcy (7 Å). However, the weak interaction of the pterin ring, the orientation of the bonds between this moiety and the *p*-aminobenzoate ring, and the empty volume between this position and the zinc atom suggests that the pterin ring can rotate easily to bring the methyl group in a close location to Hcy. This rotation could occur without moving the polyglutamate chain that plays like an anchor.

In summary, the present work describes the first three-dimensional structures of a cobalamin-independent Met synthase. Co-crystallization with either Hcy or Met and ternary complexes with folate substrates led to the identification of the zinc, Hcy, and CH_3-H_4PteGlu$_n$ binding sites. Additional work is now needed to determine (i) how the sulfur atom of Hcy is activated and (ii) how the thiolate further reacts with CH_3-H_4PteGlu$_n$. In particular, the role of phosphate that is essential for catalysis (24, 25) must be elucidated.

REFERENCES

1. Gonzalez, J. C., Banerjee, R. V., Huang, S., Sumner, J. S., and Matthews, R. G. (1992) *Biochemistry* **31,** 6045–6056
2. Matthews, R. G. (2001) *Acc. Chem. Res.* **34,** 681–689
3. Kacprzak, M. M., Lewandowska, I., Matthews, R. G., and Paszewski, A. (2003) *Biochem. J.* **376,** 517–524
4. Ravanel, S., Block, M. A., Rippert, P., Jabrin, S., Curien, G., Rebeille, F., and Douce, R. (2004) *J. Biol. Chem.* **279,** 22548–22557
5. Sunden, S. L., Renduchintala, M. S., Park, E. I., Miklasz, S. D., and Garrow, T. A. (1997) *Arch. Biochem. Biophys.* **345,** 171–174
6. Incharoensakdi, A., and Waditee, R. (2000) *Curr. Microbiol.* **41,** 227–231
7. Neuhierl, B., Thanbichler, M., Lottspeich, F., and Bock, A. (1999) *J. Biol. Chem.* **274,** 5407–5414
8. Ranocha, P., Bourgis, F., Ziemak, M. J., Rhodes, D., Gage, D. A., and Hanson, A. D. (2000) *J. Biol. Chem.* **275,** 15962–15968
9. Matthews, R. G., and Goulding, C. W. (1997) *Curr. Opin. Chem. Biol.* **1,** 332–339
10. Evans, J. C., Huddler, D. P., Jiracek, J., Castro, C., Millian, N. S., Garrow, T. A., and Ludwig, M. L. (2002) *Structure (Lond.)* **10,** 1159–1171
11. Gonzalez, B., Pajares, M. A., Martinez-Ripoll, M., Blundell, T. L., and Sanz-Aparicio, J. (2004) *J. Mol. Biol.* **338,** 771–782
12. Evans, J. C., Huddler, D. P., Hilgers, M. T., Romanchuk, G., Matthews, R. G., and Ludwig, M. L. (2004) *Proc. Natl. Acad. Sci. U. S. A.* **101,** 3729–3736
13. Zhou, Z. S., Peariso, K., Penner-Hahn, J. E., and Matthews, R. G. (1999) *Biochemistry* **38,** 15915–15926
14. Peariso, K., Zhou, Z. S., Smith, A. E., Matthews, R. G., and Penner-Hahn, J. E. (2001) *Biochemistry* **40,** 987–993
15. Roth, M., Carpentier, P., Kaïkati, O., Joly, J., Charrault, P., Pirocchi, M., Kahn, R., Fanchon, E., Jacquamet, L., Borel, F., Bertoni, A., Israel-Gouy, P., and Ferrer, J.-L. (2002) *Acta Crystallogr. Sect. D Biol. Crystallogr.* **58,** 805–814
16. Kabsch, W. (1993) *J. Appl. Crystallogr.* **26,** 795–800
17. Terwilliger, T. C., and Berendzen, J. (1999) *Acta Crystallogr. Sect. D Biol. Crystallogr.* **55,** 849–861
18. Terwilliger, T. C. (1999) *Acta Crystallogr. Sect. D Biol. Crystallogr.* **55,** 1863–1871
19. Jones, T. A., Zou, J.-Y., Cowan, S. W., and Kjeldgaard, M. (1993) *Acta Crystallogr. Sect. A* **49,** 148–157
20. Brunger, A. T., Adams, P. D., Clore, G. M., DeLano, W. L., Gros, P., Grosse-Kunstleve, R. W., Jiang, J.-S., Kuszewski, J., Nilges, N., Pannu, N. S., Read, R. J., Rice, L. M., Simonson, T., and Warren, G. L. (1998) *Acta Crystallogr. Sect. D Biol. Crystallogr.* **54,** 905–921
21. Yeates, T. O. (1997) *Methods Enzymology* **276,** 344–358
22. Kraulis, P. J. (1991) *J. Appl. Crystallogr.* **24,** 946–950
23. Fu, T.-F., Scarsdale, J. N., Kazanina, G., Schirch, V., and Wright, H. T. (2003) *J. Biol. Chem.* **278,** 2645–2653
24. Eckermann, C., Eichel, J., and Schröder, J. (2000) *Biol. Chem.* **381,** 695–703
25. Whitfield, C. D., Steers, E. J., Jr., and Weissbach, H. (1970) *J. Biol. Chem.* **245,** 390–401
26. Whitfield, C. D., and Weissbach, H. (1970) *J. Biol. Chem.* **245,** 402–409
27. Schröder, I., and Thauer, E. K. (1999) *Eur. J. Biochem.* **263,** 789–796